Applied Physics Letters

RESEARCH ARTICLE | MAY 23 2022

Interstitial proton transport through defective MXenes

Archith Rayabharam ; N. R. Aluru

Appl. Phys. Lett. 120, 211601 (2022)
https://doi.org/10.1063/5.0098709

AIP Publishing

Applied Physics Letters ARTICLE scitation.org/journal/apl

Interstitial proton transport through defective MXenes

Cite as: Appl. Phys. Lett. **120**, 211601 (2022); doi: 10.1063/5.0098709
Submitted: 25 February 2022 · Accepted: 12 May 2022 ·
Published Online: 23 May 2022

Archith Rayabharam[1] and N. R. Aluru[2,a)]

AFFILIATIONS

[1]Department of Mechanical Science and Engineering, University of Illinois at Urbana-Champaign, Illinois 61820, USA
[2]Walker Department of Mechanical Engineering, Oden Institute for Computational Engineering and Sciences, The University of Texas at Austin, Austin, Texas 78712, USA

[a)]Author to whom correspondence should be addressed: aluru@utexas.edu

ABSTRACT

Proton transport across nanometer-thick membranes in an aqueous medium is important for applications in energy and molecular sieving. Recently, Hu *et al.* [Nature **516**(7530), 227–230 (2014)] experimentally demonstrated proton tunneling through 2D materials like graphene and hexagonal boron nitride, opening up a wide range of applications in hydrogen-based technologies such as fuel cells. Here, we demonstrate proton transport in an aqueous medium across a 2D cubic Ti_2C membrane, a representative defective MXene, from *ab initio* molecular dynamics simulations. We observe bidirectional translocation of protons, which occurs through the interstitial vacancies in the surface. We show from our simulations that water dissociates on the membrane and the dissociated proton moves into the interstitial sites in the membrane. The proton hops from interstitial-to-interstitial and transports across the membrane. We also show that this interstitial proton transport is associated with an induced electric field that is modulated with bidirectional transport of protons across the membrane.

MXenes ($M_{n+1}X_n$) are an important class of 2D materials currently being explored for various applications in electronics, catalysis, energy storage, and optics.[2] For instance, it has been shown that a wide variety of ions can spontaneously intercalate between layers of Trititanium dicarbide (Ti_3C_2) and act as capacitors, enabling them to be used as energy storage devices.[3] MXenes consist of transition metal carbides or nitrides, where metals usually have multiple oxidation states. This enables the control of the stoichiometry of "X," which leads to interesting chemical properties. In addition, the transition metals at the interface have free electrons, which enable these surfaces to act as excellent catalysts. For example, the activation energy for water dissociation on transition metal carbides ranges from 0.05 to 0.4 eV,[4] which makes water dissociation practically spontaneous once it is adsorbed on the surface.

Proton conduction has been widely studied due to its applications in fuel cells and gas separation membranes.[5] The mechanism for conduction in solids is starkly different when compared to water, where proton transport occurs primarily through the Grotthuss Mechanism.[6] In most solids, a proton has to physically move from atom-to-atom or interstitial-to-interstitial in order to move through the material. In addition, proton conductors consist of oxides, where oxygens act as proton hosts and the proton hops from oxygen to oxygen.[7] Proton conduction is particularly fast in perovskite oxides,[8] where the activation energy for proton transport is small. Recently, Hu *et al.* experimentally demonstrated a new mechanism in which protons can transport through 2D membranes, where protons quantum mechanically tunnel through a single layer graphene and hexagonal boron nitride (hBN) membranes, but not through thicker membranes such as MoS_2.[1]

In this Letter, we use *ab initio* molecular dynamics (AIMD) simulations to demonstrate proton transport in an aqueous medium, through interstitial sites in a 2D cubic Ti_2C membrane. This membrane is a representative defective MXene and has titanium atoms occupying a face-centered cubic lattice, with 50% of the centers of the cubes occupied by carbon atoms. We chose Ti_2C because it has a small activation energy barrier of 0.09 eV for dissociation of water into H^+ and OH^-.[4] Even though we use 2D cubic Ti_2C to demonstrate proton transport, the method presented here can be used for other surfaces with natural or artificial interstitial sites. For example, in the supplementary material, Fig. S1, we demonstrate proton transport in 1-T phase of 2D Ti_2C with carbon vacancy defects.

2D cubic Ti_2C has preexisting interstitial vacancies in its surface. The side, top, and isometric views of such a membrane are shown in Fig. 1(a), where the polyhedra marking the bonds between carbon and

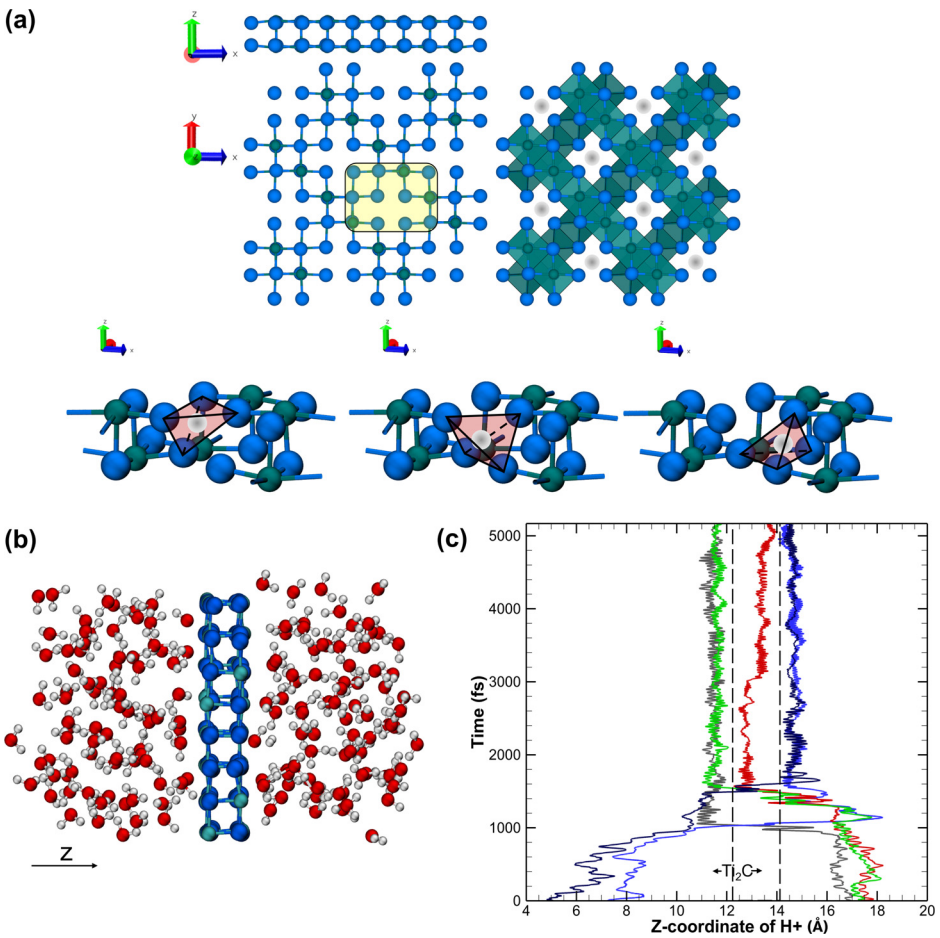

FIG. 1. (a) 2D cubic Ti_2C. Side and top views of 2D cubic Ti_2C are shown. The polyhedral formed by carbon and titanium atoms can be visualized on the right in teal. Interstitial sites can be seen as gray circles. For clarity, the yellow shaded region has been zoomed in to show the interstitial sites, each formed by four titanium atoms (red shaded regions), in an isometric view. The gray circles are virtual atoms, which mark the interstitial sites where a proton can temporarily reside. Only Ti–C bonds are shown in the membrane for easy visualization. Titanium is shown in blue, carbon in teal, oxygen in red, and hydrogen in white. (b) System for observing H^+ translocation through 2D Ti_2C. Reservoir of water on either side of a 2D-Ti_2C (cubic) membrane, which has interstitial sites available for H^+ to transport through. Only Ti–C and O–H bonds are shown for clarity. (c) Evolution of z-coordinate of H^+ ions with respect to time. Five sample trajectories of H^+ ions, which translocate through the membrane, are shown. Black dashed lines indicate the boundary of the membrane. Two of the H^+ ions translocate from the left reservoir to right (blue, dark blue) and two from right to left (green, dark green). One of the H^+ ions (red) gets trapped in the interstitial sites and remains in there until the end of the simulation.

titanium are indicated in teal. Gray circles in the top view of the lattice indicate the interstitial sites. For clarity, the yellow shaded region in the top view has been zoomed in to show the interstitial sites in the form of 3 tetrahedrons, the corners of which are marked by titanium atoms. Virtual atoms (gray) have been placed inside these tetrahedrons to mark the locations where protons can reside in the interstitial sites.

The system studied to demonstrate proton transport through a 2D cubic Ti_2C membrane is shown in Fig. 1(b) and consists of two reservoirs of water separated by the membrane. Water first gets adsorbed on the surface and forms a transient bond with one of the titanium atoms. The bond between Ti and O is expected to be ionic, with approximately 60% ionic character. This value is calculated from Pauling's empirical equation to estimate the ionic character from electronegativity differences between a pair of atoms.[9] Due to the small activation energy barrier for dissociation of water on this surface,[4] the adsorbed molecule quickly dissociates into H^+ and OH^- ions. Due to random thermal motion, the dissociated proton can move into one of the nearby interstitial vacancies. Though it is likely that the proton comes back into the initial reservoir, in some cases, it has enough energy to translocate to the other side. The energy required for translocation of proton to the other side of the membrane needs to be larger than 0.41 eV. Figure 1(c) shows the time evolution of the z-coordinate of five H^+ ions formed due to dissociation of water on the surface. As we can see from the green (dark and light) and blue (dark and light) lines, translocation of H^+ ions occurs in both directions and after translocation has occurred, and the ions prefer to stay close to the surface, interacting with the OH^- ions adsorbed on the titanium atoms on the surface. In a few cases, a proton gets trapped in the interstitial sites and is unable to escape. The z-coordinate of one of these protons is shown in red in Fig. 1(c).

An interesting way of transporting protons in an aqueous medium across a 2D Ti_2C membrane is observed from the AIMD simulations, and the mechanism of how this occurs is shown in Fig. 2. The initial configuration consists of the 2D Ti_2C membrane, and 1 water molecule placed 3 Å away from the surface. Water gets adsorbed on the surface at around 217 fs of simulation time (t). Then, energy minimization occurs where one of the hydrogen atoms of water moves closer to one of the interstitial sites (t = 703 fs). To better visualize the location of the hydrogen atom, virtual Ti–H bonds are shown in the figure, with a maximum length threshold of 2.2 Å, and the titanium atoms around the interstitial sites are numbered. As the simulation continues, water dissociates into H^+ and OH^- with an energy change (ΔE) of 0.18 eV. The H^+ ion moves into the interstitial site and OH^- forms a bond with titanium atom numbered as 1 (^{1}Ti). The dissociated OH^- ion tends to jump from titanium atom-to-titanium atom on the

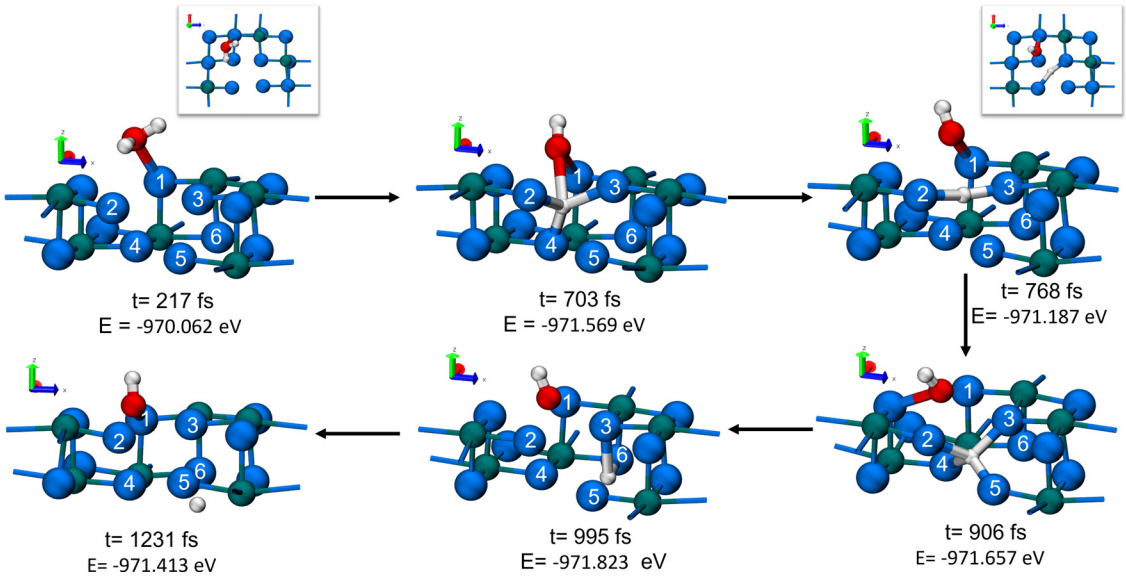

FIG. 2. Mechanism for H^+ translocation through 2D-Ti_2C. The trajectory of a water molecule on the membrane is shown as a function of time. The closest Ti atoms to the proton are shown through bonds to visualize the location of the proton, along with numbered Ti atoms to show how the bonding between Ti–H changes with time. The time at which the snapshots are taken and the corresponding energy of the system at that time are shown below each configuration. The inset snapshots show the top views for the corresponding snapshot, to aid in visualizing the in-plane location of the proton. Only Ti–C bonds are shown in the membrane for clarity. Titanium is shown in blue, carbon in teal, oxygen in red, and hydrogen in white.

surface, whereas the H^+ ion hops from one interstitial to other. For instance, between 906 and 995 fs, we see that the H^+ ion hops between two adjacent sites, first bonded to four titanium atoms ^{2}Ti, ^{3}Ti, ^{4}Ti, and ^{5}Ti at 906 fs and to titanium atoms ^{3}Ti and ^{6}Ti at 995 fs. Eventually, the H^+ ion comes out of the other side of the surface, after 1231 fs of total simulation time. In order to completely be free from the influence of the lower surface, the proton needs an additional 0.41 eV of energy. The induced electric field across the membrane (discussed in the next paragraph) can be one of the sources for this additional energy. We find that the proton goes through the membrane by hopping from a minimum energy location (stable site) to the next and overcomes an activation energy barrier in order to do so. To get an estimate of the rate of proton translocation, the diffusion coefficient of protons in the 2D Ti_2C membrane is estimated from the energy barriers using the Harmonic Transition State Theory[10] (see the supplementary material for details) and is calculated to be 8.174×10^{-9} m^2/s. In comparison, the diffusion coefficient of a proton in water is 9.6×10^{-9} m^2/s.

Figure 3(a) shows a representative mechanism of H^+ ions translocation occurring in both directions of the membrane, and how an induced electric field is created due to the movement. As the number of H^+ ions changes with time, so does the induced electric field. A cyclical change in this induced electric field is shown, where thermal motion at 300 K would play an important role in the direction of H^+ translocation, especially at the zero induced electric field. Each translocation of a H^+ ion occurs after water gets adsorbed on the surface and dissociates. The induced electric field in an AIMD simulation of the system described in Fig. 1(a) is plotted with time in Fig. 3(a). The induced electric field is normalized with the dielectric constant of Ti_2C, the electron charge, the thickness, and the area of membrane. Thus, each proton translocation through the membrane corresponds to a change of 1 unit of the normalized induced electric field. As the simulation proceeds, we observe that the magnitude of the electric field fluctuates, and this is a feature of the bi-directional transport occurring across the membrane. In addition, the electric field changes in distinct steps corresponding to the charge of each H^+ ion translocated. The bi-directional transport of H^+ can also be explicitly seen in Fig. 3(c), where the total number of translocations occurring in either direction has been plotted with time. For the first few translocations, we observe that a proton moving from left to right is immediately followed by one moving from right to left. As the simulation proceeds, we see that the difference between the number of protons translocating from left to right (L to R) and from right to left (R to L) increases. It should be noted that to make the transport more directionally selective, we can control the initial pH difference or apply an external electric field to overcome the induced electric field generated due to the translocation.

In conclusion, we demonstrate how interstitial vacancies in a 2D material can be used to translocate protons in an aqueous medium. We obtain protons in an aqueous medium through dissociating water on the 2D cubic Ti_2C surface, a representative defective MXene. The mechanism through which proton translocations occurs has also been discussed, and it is observed that the proton translocation is bi-directional across the membrane due to the thermal motion of atoms. Finally, we show that, as protons translocate through the membrane, an electric field is induced across the membrane, which fluctuates with time, either due to random thermal motion of atoms or due to a force on the protons due to the induced electric field.

The analysis of proton transport through 2D Ti_2C has been carried out using *ab initio* molecular dynamics (AIMD) using the Vienna *Ab initio* simulation (VASP) package.[11] The Perdew–Burke–Ernzerhof (PBE)[12] exchange-correlation functional, which comes under the

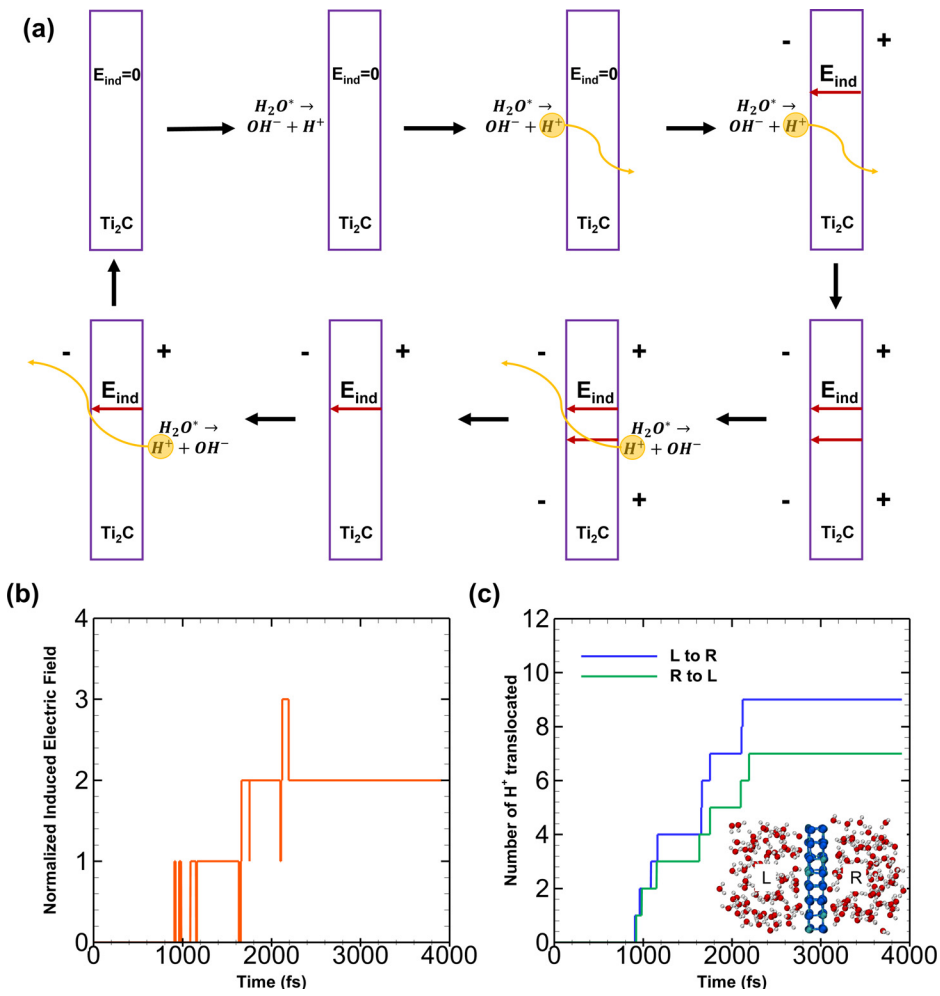

FIG. 3. (a) Induced electric field changing due to H^+ ion translocation. A representative schematic of how the induced electric field on the membrane changes when H^+ ions translocate through it. The direction and magnitude of the electric field are shown using red arrows. The corresponding magnitude of charges on each wall of the membrane is represented with charges (+ or −), where the walls of the 2D cubic Ti_2C membrane are shown in blue. Yellow arrows indicate one translocation event, either occurring from left to right or vice versa. Water adsorbed on one of the titanium atoms is indicated by H_2O^*. (b) Fluctuation of the induced electric field as a function of time: real time values of the fluctuating electric field are plotted on the y-axis with time from an AIMD simulation of the system described in Fig. 1(b). This electric field is normalized by the electron charge, the thickness of the membrane, and the area of the membrane. Water dissociating on the surface creates charged ions and a fraction of the H^+ ions generated translocate across the pore. Each H^+ ion translocating across the membrane changes the electric field by 1 unit. The discrete steps in which the electric field changes can be seen. Positive values imply that the direction of the induced electric field is from right to left. (c) Number of H^+ ions translocated: due to the fluctuating electric field and thermal oscillations, H^+ translocation is observed through both left to right (L to R) and right to left (R to L) directions. The selectivity for achieving unidirectional transport of protons can be controlled by the pH difference between the reservoirs or by applying additional forces on the system.

Generalized Gradient Approximation (GGA), was used and projected augmented wave (PAW) pseudopotentials[13] with an energy cutoff of 450 eV and a Gamma-point-centered k-point grid of $2 \times 2 \times 2$ were used. The system used to demonstrate the mechanism of proton transport consists of 64 titanium, 32 carbon atoms, and 1 water molecule. The water molecule in this case is initially placed 3 Å away from the surface. In order to study the energetics of proton translocation through interstitial sites, self-consistent density functional theory (DFT) simulations were performed for each of the snapshots in Fig. 2. The energy cutoff and the k-point grid used were the same as those for the AIMD simulations. The system used to analyze the number of proton translocations is shown in Fig. 1(c), which also consists of 64 titanium, 32 carbon atoms, along with 160 water molecules. 80 water molecules are placed in each reservoir. The simulation box has the dimensions $17.278 \times 17.278 \times 28$ Å^3, and a canonical or isochoric-isothermal (NVT) ensemble is used at 300 K, with a time step of 0.5 fs. Figure 1(c) is plotted by tracking the z-coordinate of five sample H^+ ions, which translocate across the membrane. The induced electric field and the number of H^+ ions translocated in Figs. 3(b) and 3(c), respectively, are calculated by tracking the z-coordinate of all the H^+ ions, and a particular ion is counted as translocated across the membrane when it moves from either left to right or right to left in Fig. 1(b).

See the supplementary material for the details on the calculation of diffusion coefficient of protons in cubic 2D Ti_2C membrane and demonstration of proton translocation in the 1-T phase of 2D Ti_2C with carbon vacancies.

This work was supported by the Center for Enhanced Nanofluidic Transport (CENT), an Energy Frontier Research Center funded by the U.S. Department of Energy, Office of Science, Basic Energy Sciences under Award No. DE-SC0019112. We also acknowledge the Texas Advanced Computing Center (TACC) at The University of Texas at Austin for providing the computing resources on Stampede2 and Frontera under the allocation Nos. TG-CDA100010 and DMR20002, respectively.

AUTHOR DECLARATIONS

Conflict of Interest

The authors have no conflicts to disclose.

Author Contributions

A.R. performed simulations and analysis and wrote the manuscript under the guidance of N.R.A.

DATA AVAILABILITY

The data that support the findings of this study are available within the article and its supplementary material.

REFERENCES

[1]S. Hu, M. Lozada-Hidalgo, F. Wang, A. Mishchenko, F. Schedin, R. R. Nair, E. Hill, D. Boukhvalov, M. Katsnelson, and R. A. Dryfe, "Proton transport through one-atom-thick crystals," Nature **516**(7530), 227–230 (2014).

[2]B. Ahmed, A. E. Ghazaly, and J. Rosen, "*i*-MXenes for energy storage and catalysis," Adv. Funct. Mater. **30**(47), 2000894 (2020); Z. Xia, Q. Huang, and S. Guo, "Recent progress on synthesis, structure and electrocatalytic applications of MXenes," FlatChem **17**, 100129 (2019); H. Kim, Z. Wang, and H. N. Alshareef, "MXetronics: Electronic and photonic applications of MXenes," Nano Energy **60**, 179–197 (2019); M. Khazaei, A. Ranjbar, M. Arai, T. Sasaki, and S. Yunoki, "Electronic properties and applications of MXenes: A theoretical review," J. Mater. Chem. C **5**(10), 2488–2503 (2017); B. Anasori, M. R. Lukatskaya, and Y. Gogotsi, "2D metal carbides and nitrides (MXenes) for energy storage," Nat. Rev. Mater. **2**(2), 16098 (2017).

[3]M. R. Lukatskaya, O. Mashtalir, C. E. Ren, Y. Dall'Agnese, P. Rozier, P. L. Taberna, M. Naguib, P. Simon, M. W. Barsoum, and Y. Gogotsi, "Cation intercalation and high volumetric capacitance of two-dimensional titanium carbide," Science **341**(6153), 1502–1505 (2013).

[4]J. D. Gouveia, A. Morales-Garcia, F. Vines, F. Illas, and J. R. Gomes, "MXenes as promising catalysts for water dissociation," Appl. Catal., B **260**, 118191 (2020).

[5]M. Yoon, K. Suh, S. Natarajan, and K. Kim, "Proton conduction in metal–organic frameworks and related modularly built porous solids," Angew. Chem., Int. Ed. **52**(10), 2688–2700 (2013); R. Haugsrud and T. Norby, "Proton conduction in rare-earth ortho-niobates and ortho-tantalates," Nat. Mater. **5**(3), 193–196 (2006); J. Gao, Y. Meng, A. Benton, J. He, L. G. Jacobsohn, J. Tong, and K. S. Brinkman, "Insights into the proton transport mechanism in TiO_2 simple oxides by *in situ* Raman spectroscopy," ACS Appl. Mater. Interfaces **12**(34), 38012–38018 (2020).

[6]N. Agmon, "The Grotthuss mechanism," Chem. Phys. Lett. **244**(5–6), 456–462 (1995).

[7]T. Norby, "Proton conduction in solids: Bulk and interfaces," MRS Bull. **34**(12), 923–928 (2009).

[8]D. Pergolesi, E. Fabbri, A. D'Epifanio, E. Di Bartolomeo, A. Tebano, S. Sanna, S. Licoccia, G. Balestrino, and E. Traversa, "High proton conduction in grain-boundary-free yttrium-doped barium zirconate films grown by pulsed laser deposition," Nat. Mater. **9**(10), 846–852 (2010).

[9]L. Pauling, *The Nature of the Chemical Bond* (Cornell University Press, Ithaca, NY, 1960).

[10]G. H. Vineyard, "Frequency factors and isotope effects in solid state rate processes," J. Phys. Chem. Solids **3**(1–2), 121–127 (1957).

[11]G. Kresse and J. Furthmüller, "Efficiency of ab-initio total energy calculations for metals and semiconductors using a plane-wave basis set," Comput. Mater. Sci. **6**(1), 15–50 (1996); G. Kresse and J. Furthmüller, "Efficient iterative schemes for ab initio total-energy calculations using a plane-wave basis set," Phys. Rev. B **54**(16), 11169 (1996).

[12]J. P. Perdew, K. Burke, and M. Ernzerhof, "Generalized gradient approximation made simple," Phys. Rev. Lett. **77**(18), 3865 (1996).

[13]G. Kresse and D. Joubert, "From ultrasoft pseudopotentials to the projector augmented-wave method," Phys. Rev. B **59**(3), 1758 (1999).